



Quasielastic neutron scattering of hydrated $\text{BaZr}_{0.90}\text{A}_{0.10}\text{O}_{2.95}$ ($\text{A}=\text{Y}$ and Sc)

Maths Karlsson^{a,b,*}, Aleksandar Matic^b, Dennis Engberg^b, Mårten E. Björketun^b, Michael M. Koza^c, Istaq Ahmed^{d,e}, Göran Wahnström^b, Lars Börjesson^b, Sten-G. Eriksson^d

^a European Spallation Source Scandinavia, Lund University, SE-221 00 Lund, Sweden

^b Department of Applied Physics, Chalmers University of Technology, SE-412 96 Göteborg, Sweden

^c Institut Laue Langevin, 6 Rue Jules Horowitz, Boite Postale 156, 38042 Grenoble, Cedex 9, France

^d Department of Chemical and Biological Engineering, Chalmers University of Technology, SE-412 96 Göteborg, Sweden

^e The ISIS Facility, STFC Rutherford Appleton Laboratory, Didcot, Oxfordshire, OX110QX, United Kingdom

ARTICLE INFO

Article history:

Received 22 June 2008

Received in revised form 7 November 2008

Accepted 9 November 2008

Keywords:

Proton conducting

Perovskite

Quasielastic neutron scattering

ABSTRACT

Proton motions in hydrated proton conducting perovskites $\text{BaZr}_{0.90}\text{A}_{0.10}\text{O}_{2.95}$ ($\text{A}=\text{Y}$ and Sc) have been investigated using quasielastic neutron scattering. The results reveal a localized motion on the ps time scale and with an activation energy of $\sim 10\text{--}30$ meV, in both materials. The temperature dependence of the total mean square displacement of the protons shows an onset of this motion at a temperature of about 300 K. The low activation energy, much lower than the activation energy for the macroscopic proton conductivity, suggests that this motion is not the rate-limiting process for the long-range proton diffusion, *i.e.* it is not linked to the two materials significantly different proton conductivities. In fact, a comparison of the QENS results with density functional theory calculations indicates that for both materials the observed motion may be ascribed to intra-octahedral proton transfers occurring close to a dopant atom.

© 2008 Elsevier B.V. All rights reserved.

1. Introduction

Hydrated acceptor-doped perovskites are known to be proton conductors in the temperature range $\sim 200\text{--}700$ °C [1]. The doping creates an oxygen-deficient structure and in a humid atmosphere water molecules dissociate into hydroxide ions, which fill the oxygen vacancies, and protons, which bond to lattice oxygen [1]. The proton conduction mechanism in these hydrated acceptor-doped perovskites can be divided into two elementary steps: (i) hydrogen-bond mediated proton transfer between adjacent oxygen, and (ii) reorientational motion of the hydroxyl group in between such transfers. In this two-stage mechanism it is only the protons that exhibit long-range diffusion while the oxygen reside on their crystallographic positions. These processes have been studied in different systems mainly using molecular dynamics simulations [2–5] and quasielastic neutron scattering (QENS) [6,7]. QENS is a particularly suitable experimental technique as it gives access to the time range $\sim 10^{-13}\text{--}10^{-9}$ s, in which these processes occur, as well as providing information about the spatial geometry of the atomic motions. In addition, the very high neutron scattering cross section of protons provides a good contrast in the experiments and enables studies of systems with a low dopant concentration, *i.e.* a low hydration degree and concomitantly few protons.

Previous QENS investigations have revealed localized motions in the ps time range, mainly interpreted as rotational motions with radii bet-

ween $r\sim 0.7$ and 1.1 Å, and with activation energies $E_a\lesssim 100$ meV [7,8]. The results have also been interpreted in more complex terms of a diffusional process of the proton, consisting of a sequence of free diffusion and trapping/escape events [6]. These studies have, however, been performed on orthorhombic perovskites, namely hydrated $\text{SrCe}_{0.95}\text{Yb}_{0.05}\text{O}_{2.95}$ and $\text{Ba}_3\text{Ca}_{1.17}\text{Nb}_{1.83}\text{O}_{8.73}$, which makes the interpretation of the data more difficult as the structure is intrinsically anisotropic and there are several non-equivalent oxygen sites for the protons in the structure. In addition, no study has addressed the question of the role of the type of dopant on the elementary steps in the conduction mechanism.

Molecular dynamics simulations on proton conducting perovskites have revealed a fast rotational motion of the protons around the line connecting the corners of the perovskite unit cell, on the ps time scale and with an activation energy less than 50 meV [2–4]. By extending the simulations to higher temperatures and pressures, also several proton transfer events within a simulation time of ~ 100 ps have been observed [3]. This process was found to be considerably dependent on the oxygen–oxygen separation, inferred by the vibrations of the oxygen sublattice [3]. In the contracted transition state, having an energy of ~ 0.41 eV, proton transfer was found to occur almost barrierless, although it was not always that the proton was transferred [3].

In the present work we investigate the proton dynamics in 10% Y- and Sc-doped BaZrO_3 , using QENS. One of the interests in this study lies in the fact that although the structures of these two perovskites are very similar, they are both cubic [9,10], their proton conductivities differ almost two orders of magnitude with the Y-doped perovskite exhibiting the highest [9].

* Corresponding author. Tel.: +46 462228861; fax: +33 476207648.
E-mail address: maths.karlsson@ill.eu (M. Karlsson).

2. Experimental

The $\text{BaZr}_{0.90}\text{A}_{0.10}\text{O}_{2.95}$ ($A=\text{Y}$ and Sc) samples, hereafter abbreviated as 10Y:BZO and 10Sc:BZO, respectively, were prepared by mixing stoichiometric amounts of BaCO_3 , ZrO_2 and $(\text{Y}/\text{Sc})_2\text{O}_3$. The oxides were heated to 800 °C overnight to remove moisture prior to weighing. Milling was performed manually using an agate mortar and a pestle. The finely ground mixtures were fired at 1000 °C for 8 h and subsequently ground and pelletized using a 13 mm diameter die under a pressure of 8 tons. The pellets were sintered at 1200 °C in air for 72 h. After sintering, the pellets were reground, compacted, and refired at 1500 °C for 48 h. Finally, the pellets were finely reground to powders. The charging with protons was performed by annealing the powder samples at ~300 °C under a flow (12 ml/min) of Ar saturated with water vapor at 76 °C for 10 days. X-ray diffraction measurements, performed at ambient temperature on a Siemens D500 powder diffractometer ($\text{CuK}\alpha_1=1.5406$ Å), revealed a cubic structure of both hydrated materials, which is in agreement with other investigations [9,10].

The QENS experiments were performed at the time-of-flight spectrometer IN6 at the Institut Laue Langevin in Grenoble (France), using neutrons with a wavelength of 5.1 Å, yielding an energy resolution of 100 μeV (FWHM) and a Q -range 0.26–1.9 Å^{-1} . See ref. [11] for a further description of the spectrometer. The Q -dependent spectra were summed into 14 groups to increase the statistics. Spectra were measured at 2, 250, 300, 380, 430, 465 and 495 K for 10Y:BZO, and at 2, 380, 430, 465 and 495 K for 10Sc:BZO, and the integration time for each spectrum was 4 h. The 2 K measurements were used as resolution functions in the data analysis, since at this low temperature all diffusional motions of the protons are frozen-in, and the scattered intensity is solely elastic. The samples were loaded in flat vacuum tight Al-containers, which were coated on the inside with a 100 nm thick layer of Pt to avoid corrosion. The sample thickness was chosen to 6 mm, which yielded a total scattering of approximately 10%. For 10Y:BZO, the total coherent, total incoherent, and total absorption cross-sections for neutrons are 22.7, 8.2 and 1.4 barns, respectively, while for 10Sc:BZO, these values are 24.2, 8.6 and 4.1 barns. It should be noted that although the total incoherent scattering is only about one fourth of the total scattering of neutrons, nearly all incoherent scattering (~98% for 10Y:BZO and ~93% for 10Sc:BZO) comes from the protons. Measurements were performed in transmission geometry with the sample aligned at 135° in respect to the incoming neutron beam in a cryofurnace. This way self attenuation effects due to the sample geometry were strongly suppressed in the range of scattering angles (10–115°) covered by the IN6 multidetector. The applied incident wavelength of 5.1 Å does not allow the scattering from Bragg-reflections of the purely coherently scattering container material, aluminum. In the energy range of interest, -2 to 2 meV, the monitored signal is therefore almost free from any temperature dependent parasitic scattering of the sample environment. Therefore, the background scattering has been measured with high accuracy at 380 K. The spectrum of a vanadium standard was used to correct for the detector efficiency.

3. Theoretical background

In a QENS experiment one obtains the dynamic structure factor, $S(Q, \omega)$, which gives the probability that an incident neutron is scattered by the sample with a momentum transfer $\hbar Q$ and an energy transfer $\hbar\omega$. In our analysis we have modeled $S(Q, \omega)$ with the following scattering function

$$S_q(Q, \omega) = b(Q) \cdot \delta(\hbar\omega) + \frac{1}{\pi} \frac{a_L(Q) \cdot \Delta\omega(Q)}{(\hbar\omega)^2 + [\Delta\omega(Q)]^2} + c(Q) + d(Q) \cdot (\hbar\omega). \quad (1)$$

Here, the first term describes the elastic scattering from those atoms that move too slow to be resolved in the experiment ($b(Q)$ is a Q -dependent constant and $\delta(\hbar\omega)$ is a delta function). The second term,

which is the quasielastic term and appears as a broadening of the elastic peak, accounts for stochastic motions (translational and reorientational), which result in a small energy loss/gain of the incident neutrons. One should note that only protons are expected to move on the time scale that the IN6 spectrometer can resolve (~10⁻¹³ to 10⁻¹⁰ s), which facilitates the analysis. The quasielastic scattering is described by a Lorentzian with amplitude $a_L(Q)$ and width $\Delta\omega(Q)$ (HWHM), while $c(Q)$ and $d(Q)$ are parameters of a sloping background. One should here note that even though one can expect several types of proton motions on the time scale of what this spectrometer can resolve, the model we use only gives information about one type of proton motion, or an average of several types of proton motions. Indeed, in previous QENS investigations [6–8] of proton dynamics in hydrated perovskites more sophisticated, and perhaps more physically appealing, models have been used to describe the proton motion. However, due to the low scattering contrast in our measurements we would not resolve more details of the proton motion than we do with Eq. (1). Thus, more elaborate models cannot be justified.

The measured scattering function, $S_{\text{meas}}(Q, \omega)$, is a convolution of the real scattering function, $S(Q, \omega)$, and the resolution function of the instrument, $R(Q, \omega)$, i.e.

$$S_{\text{meas}}(Q, \omega) = S(Q, \omega) \otimes R(Q, \omega). \quad (2)$$

Thus, the modeled scattering function in Eq. (1) is convoluted with the resolution function in the data analysis.

The Q -dependences of $\Delta\omega$ and a_L contain information about the relaxation time and spatial geometry of the proton dynamics. For instance, for a long-range diffusional process and for sufficiently small Q -values, the quasielastic width follows a characteristic Q^2 -dependence according to $\Delta\omega = \hbar D Q^2$, where D is the diffusion constant [12]. For a local process, e.g. a rotational motion, $\Delta\omega$ is practically Q -independent and is related to the relaxation time τ through $\tau = \hbar/\Delta\omega$ [12]. Here one should note that before analyzing the Q -dependence of the quasielastic intensities, a_L , these need to be corrected for the overall decrease in scattering intensity due to the Debye-Waller factor, that accounts for the harmonic (vibrational) motions. The total scattering can be written as

$$S(Q, \omega) = e^{-\langle u^2 \rangle_{\text{harm}} Q^2} S_q(Q, \omega) \quad (3)$$

where $\langle u^2 \rangle_{\text{harm}}$ is the harmonic mean square displacement of all atoms in the material. Thus, also the mean square displacement is needed for the full analysis of the experimental data. Following a customary route in the analysis of QENS data, the total mean square displacement $\langle u^2 \rangle$,

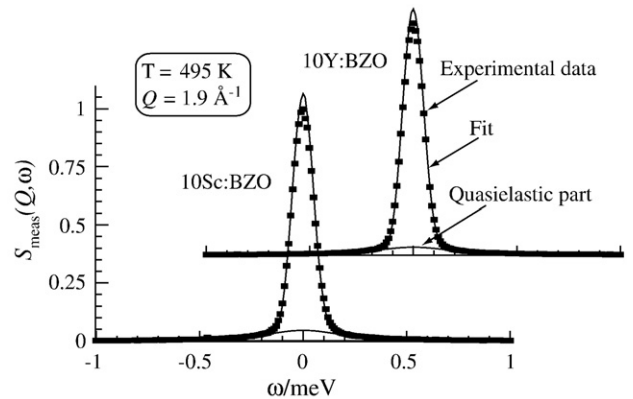


Fig. 1. $S_{\text{meas}}(Q, \omega)$ of 10Y:BZO and 10Sc:BZO at $Q=1.9$ Å^{-1} and for $T=495$ K. The solid lines represent fits to the experimental data (markers) according to Eq. (1). The spectra have been normalized in intensity to unity for easier comparison.

Download English Version:

<https://daneshyari.com/en/article/1297029>

Download Persian Version:

<https://daneshyari.com/article/1297029>

[Daneshyari.com](https://daneshyari.com)